Journal of
Mechanics of
Materials and Structures

POLARIZATION APPROXIMATIONS FOR ELASTIC MODULI OF ISOTROPIC MULTICOMPONENT MATERIALS

Duc Chinh Pham, Nguyen Quyet Tran and Anh Binh Tran

Volume 12, No. 4 July 2017

msp

JOURNAL OF MECHANICS OF MATERIALS AND STRUCTURES
Vol. 12, No. 4, 2017
dx.doi.org/10.2140/jomms.2017.12.391

msp

POLARIZATION APPROXIMATIONS FOR ELASTIC MODULI OF ISOTROPIC MULTICOMPONENT MATERIALS

DUC CHINH PHAM, NGUYEN QUYET TRAN AND ANH BINH TRAN

Polarization approximations (PA) are proposed for the macroscopic elastic moduli of d-dimensional ($d = 2$ or 3) isotropic multicomponent materials. Specifically we use Hashin–Shtrikman-type polarization trial fields, which were constructed earlier from the minimum energy principles to bound the effective moduli of the composites, as the approximate solutions to the field equations. The approximations contain free reference parameters, which can be found analytically, numerically, or experimentally, from the reference effective moduli at dilute and/or finite volume proportions of the component materials. In the basic one-point reference parameter version, the approximations should obey Hashin–Shtrikman (HS) bounds for all the ranges of the volume proportions of the component materials. In the refined versions involving variable reference parameters to improve the accuracy of the scheme, the approximations satisfy HS bounds over the ranges of components' volume proportions between the extreme reference points. We provide numerous numerically and experimentally based examples to illustrate the applications of the proposed approach.

1. Introduction

Many natural and industrial materials are multicomponent with complex and irregular microstructure. Often only limited definite qualitative information about the composites, e.g., the properties and volume proportions of the component materials, is available. Still, the measured macroscopic moduli of many practical composites appear relatively definite (with small variation), and that encourages us to construct simple estimations of the moduli for practical uses. A mathematically rigorous approach to the problem is to construct the upper and lower bounds of the effective moduli using variational formulations [Hashin and Shtrikman 1963; Walpole 1966; Willis 1977; Pham 1993; 2012; 2014; Milton 2002; Torquato 2002]. Narrowing the bounds requires multipoint correlation information about the microgeometries of the composites that is difficult to collect and incorporate into the construction of the bounds. Alternatively, effective medium approximation (EMA) schemes have been developed for practical estimates of composites' macroscopic moduli [Mori and Tanaka 1973; Christensen 1979; Norris 1989; Mura 1987; Phan-Thien and Pham 2000; Torquato 2002; Nogales and Böhm 2008; Klusemann et al. 2012; Franciosi et al. 2011; Mogilevskaya et al. 2012; Kushch et al. 2013; Sevostianov and Kachanov 2014] (among many others). Many classical EMAs, such as the self-consistent, Mori–Tanaka, differential ones are based on the dilute solutions for the inhomogeneities of some idealistic forms suspended in an infinite matrix (the Eshelby problem [1957]) and are then developed into the forms that can predict the effective moduli of the composites over a range of volume proportions of the inhomogeneities. All EMAs converge at the dilute limit of the inclusions but diverge from each other at large volume proportions of the included

Keywords: isotropic composite material, macroscopic elastic moduli, polarization approximation, reference parameter.

phases. To get better approximations, additional information about a particular composite, such as the effective moduli at some inclusions' volume proportion points, if available, should be included into an EMA. In this work we propose novel polarization approximations which can offer that flexibility. The idea was first introduced in our work [Tran and Pham 2015] for practical uniaxial circular fiber composites. We constructed certain polarization approximations for the effective elastic transverse (two-dimensional) bulk and shear moduli, among other moduli, of the transverse-isotropic composites, with numerical illustrations. In this work we generalize the idea as follows: polarization approximations are derived for the elastic bulk and shear moduli of isotropic three-dimensional composites and given in convenient forms valid for those in general d dimensions. General forms of the inhomogeneities (not just the circular one), with both numerical and experimental references from various composites, are considered. To improve the approximations, variable reference parameter for the approximation is proposed to take into account more information about a composite.

In Section 2, the polarization trial fields that were constructed earlier from the minimum energy principles to bound the effective elastic moduli will be used to derive the polarization approximations. Those approximations depend on certain free reference parameters. Those free (generally variable) parameters are determined analytically, numerically, or experimentally, using certain reference macroscopic moduli in subsequent sections, which are then followed by the conclusion (Section 6).

2. Polarization approximations

Let us consider a representative volume element (RVE) V in d-dimensional Euclidean space ($d = 2, 3$) of a macroscopically isotropic multicomponent. The material consists of n isotropic components occupying regions $V_\alpha \subset V$ of volumes v_α and having elastic moduli K_α and μ_α ($\alpha = 1, \ldots, n$ and the volume of V is assumed to be unity). The effective elastic moduli $\boldsymbol{C}^{\text{eff}} = \boldsymbol{T}(K^{\text{eff}}, \mu^{\text{eff}})$ of the isotropic composite may be defined via the minimum energy principle [Pham 1993; 2012; 2014]

$$\boldsymbol{\varepsilon}^0 : \boldsymbol{C}^{\text{eff}} : \boldsymbol{\varepsilon}^0 = \inf_{\langle \boldsymbol{\varepsilon} \rangle = \boldsymbol{\varepsilon}^0} \int_V \boldsymbol{\varepsilon}(\boldsymbol{x}) : \boldsymbol{C}(\boldsymbol{x}) : \boldsymbol{\varepsilon}(\boldsymbol{x})\, d\boldsymbol{x}, \tag{1}$$

for all macroscopic constant strain tensors $\boldsymbol{\varepsilon}^0$, where $\boldsymbol{C}(\boldsymbol{x})$ is the fourth-rank stiffness tensor, $\boldsymbol{T}$ is the isotropic fourth-rank tensor with components

$$T_{ijkl}(K, \mu) = K\delta_{ij}\delta_{kl} + \mu\left(\delta_{ik}\delta_{jl} + \delta_{il}\delta_{jk} - \frac{2}{d}\delta_{ij}\delta_{kl}\right), \tag{2}$$

the trial compatible strain field is expressed through the displacement field $\boldsymbol{u}(\boldsymbol{x})$ as

$$\boldsymbol{\varepsilon}(\boldsymbol{x}) = \tfrac{1}{2}[\nabla \boldsymbol{u}(\boldsymbol{x}) + (\nabla \boldsymbol{u})^T(\boldsymbol{x})], \tag{3}$$

and $\langle \cdot \rangle$ means the volume average on V.

The effective elastic moduli may also be defined via the minimum complementary energy principle [Pham 1993; 2012; 2014]

$$\boldsymbol{\sigma}^0 : (\boldsymbol{C}^{\text{eff}})^{-1} : \boldsymbol{\sigma}^0 = \inf_{\langle \boldsymbol{\sigma} \rangle = \boldsymbol{\sigma}^0} \int_V \boldsymbol{\sigma}(\boldsymbol{x}) : \boldsymbol{C}^{-1}(\boldsymbol{x}) : \boldsymbol{\sigma}(\boldsymbol{x})\, d\boldsymbol{x}, \tag{4}$$

for all macroscopic constant stress tensors $\boldsymbol{\sigma}^0$, where the trial stress field $\boldsymbol{\sigma}(\boldsymbol{x})$ should satisfy equilibrium equations in V

$$\nabla \cdot \boldsymbol{\sigma}(\boldsymbol{x}) = \mathbf{0}. \tag{5}$$

Note that the two-dimensional bulk modulus K here in the two-dimensional Cartesian coordinates $\{x_1, x_2\}$ is defined by $\sigma_{11} + \sigma_{22} = 2K(\varepsilon_{11} + \varepsilon_{22})$. Hence, it is related to the usual three-dimensional bulk modulus designated specifically here as $\widetilde{K}$: $K = \widetilde{K} + \mu/3$ in the plane strain case and $K = 9\widetilde{K}\mu/(3\widetilde{K} + 4\mu)$ in the plane stress case.

We consider the 3D case in the following equations, from (6) to (10). To find the upper correlation bounds on K^{eff} and μ^{eff} for isotropic three-dimensional composites, instead of directly optimizing the energy expression of the complex problem (1), we [Pham 1993; 2014] have optimized a "principal part" of it and came to a Hashin–Shtrikman-type polarization trial strain field

$$\varepsilon_{ij} = \varepsilon^0_{ij} + \frac{3K_0 + \mu_0}{\mu_0(3K_0 + 4\mu_0)} \sum_{\alpha=1}^{n} p^\alpha_{kl} \psi^\alpha_{,ijkl} - \frac{1}{2\mu_0} \sum_{\alpha=1}^{n} (p^\alpha_{mi} \varphi^\alpha_{,jm} + p^\alpha_{mj} \varphi^\alpha_{,im}), \tag{6}$$

where K_0 and μ_0 are some free positive parameters (called the elastic moduli of a reference material in Hashin–Shtrikman approach); indices after a comma designate differentiation with respect to the corresponding Cartesian coordinates; conventional summation on repeated indices (from 1 to 3) is assumed; p^α_{kl} are the components of the second-order tensor $\boldsymbol{p}^\alpha$, which is referred to as the polarization field in the Hashin–Shtrikman (HS) approach

$$\begin{aligned}
&\boldsymbol{p}^\alpha = \left\{ \boldsymbol{I} - (\boldsymbol{C}^\alpha + \boldsymbol{C}^*)^{-1} : \left[\sum_{\beta=1}^{n} v_\beta (\boldsymbol{C}^\beta + \boldsymbol{C}^*)^{-1} \right]^{-1} \right\} : (\boldsymbol{C}^0 + \boldsymbol{C}^*) : \boldsymbol{\varepsilon}^0, \\
&\boldsymbol{C}^0 = \boldsymbol{T}(K_0, \mu_0), \qquad \boldsymbol{I} = \boldsymbol{T}\left(\tfrac{1}{3}, \tfrac{1}{2}\right), \quad \boldsymbol{C}^\alpha = \boldsymbol{T}(K_\alpha, \mu_\alpha), \\
&\boldsymbol{C}^* = \boldsymbol{T}(K_*, \mu_*), \quad K_* = \tfrac{4}{3}\mu_0, \qquad \mu_* = \mu_0 \frac{9K_0 + 8\mu_0}{6K_0 + 12\mu_0};
\end{aligned} \tag{7}$$

$\varphi^\alpha(\boldsymbol{x})$ and $\psi^\alpha(\boldsymbol{x})$ are harmonic and biharmonic potentials originated from the expression of the Green function for the 3D elastic infinite medium (which satisfy equations $\nabla^2 \varphi^\alpha(\boldsymbol{x}) = \nabla^4 \psi^\alpha(\boldsymbol{x}) = \delta_{\alpha\beta}$ for $\boldsymbol{x} \in V_\beta$, where $\delta_{\alpha\beta}$ is the usual Kronecker delta). Since the phases are assumed to be distributed isotropically in the material space, one has [Walpole 1966; Christensen 1979; Pham 1993]

$$\begin{aligned}
\langle \varphi^\beta_{,ij} \rangle_\alpha &= \frac{1}{v_\alpha} \int_{V_\alpha} \varphi^\beta_{,ij} \, d\boldsymbol{x} = \tfrac{1}{3} \delta_{ij} \delta_{\alpha\beta}, \\
\langle \psi^\beta_{,ijkl} \rangle_\alpha &= \frac{1}{v_\alpha} \int_{V_\alpha} \psi^\beta_{,ijkl} \, d\boldsymbol{x} = \tfrac{1}{15} (\delta_{ij}\delta_{kl} + \delta_{il}\delta_{jk} + \delta_{ik}\delta_{jl}) \delta_{\alpha\beta},
\end{aligned} \tag{8}$$

where $\langle \cdot \rangle_\alpha = (1/v_\alpha) \int_{V_\alpha} \cdot \, d\boldsymbol{x}$ designates the volume average on V_α, while $\langle \cdot \rangle = \int_V \cdot \, d\boldsymbol{x}$ is the volume average on the whole representative volume element V.

In Pham's [1993; 2014] upper-bound approach, the upper correlation bounds on K^{eff} and μ^{eff} obtained from (1) with the trial field (6)–(7) contain the three-point correlation information about the microgeometry of a composite, and K_0 and μ_0 should be chosen to minimize the upper bounds. K_0 and μ_0 should lie within the extreme values of K_α and μ_α. The trial field of formal type (6) has also been obtained by [Walpole 1966; Willis 1977; Christensen 1979], using other approaches.

On the other side, to find the lower correlation bounds on the effective moduli, instead of directly optimizing the complementary energy expression of (4), [Pham 1993; 2014] optimized a "principal part" of it and obtained the polarization trial stress field

$$\begin{aligned}
&\boldsymbol{\sigma}(\boldsymbol{x}) = \boldsymbol{\sigma}^0 - \boldsymbol{C}^0 : [\boldsymbol{\varepsilon}'(\boldsymbol{x}) + \boldsymbol{q}(\boldsymbol{x})], \quad \hat{\boldsymbol{q}}^\alpha = \boldsymbol{C}^0 : \boldsymbol{q}^\alpha,\\
&\varepsilon'_{ij}(\boldsymbol{x}) = \frac{3K_0 + \mu_0}{\mu_0(3K_0 + 4\mu_0)} \sum_{\alpha=1}^{n} \hat{q}^\alpha_{kl} \psi^\alpha_{,ijkl} - \frac{1}{2\mu_0} \sum_{\alpha=1}^{n} (\hat{q}^\alpha_{mi} \varphi^\alpha_{,jm} + \hat{q}^\alpha_{mj} \varphi^\alpha_{,im}),\\
&\boldsymbol{q}^\alpha = \left\{ \boldsymbol{I} - [(\boldsymbol{C}^\alpha)^{-1} + (\boldsymbol{C}^*)^{-1}]^{-1} : \left[\sum_{\beta=1}^{n} v_\beta [(\boldsymbol{C}^\beta)^{-1} + (\boldsymbol{C}^*)^{-1}]^{-1} \right]^{-1} \right\} : [(\boldsymbol{C}^0)^{-1} + (\boldsymbol{C}^*)^{-1}] : \boldsymbol{\sigma}^0,
\end{aligned} \tag{9}$$

where $\boldsymbol{q}(\boldsymbol{x}) = \boldsymbol{q}^\alpha$ when $\boldsymbol{x} \in V_\alpha$; other notations are similar to those in (7) and (8). In the lower-bound approach, K_0 and μ_0 should be chosen to maximize the lower bounds on K^{eff} and μ^{eff} obtained from (4) with the trial field (9). K_0 and μ_0 should lie within the extreme values of K_α and μ_α.

Extracting the correlation information on a particular composite's microgeometry needed for the three-point correlation bounds in [Pham 1993] is costly. To avoid this, we directly use the "optimal" polarization trial fields (6) or (9) as the approximate solution fields on the RVE to construct the polarization approximations for the effective elastic moduli. Following the approach of [Tran and Pham 2015] in the two-dimensional case, one may use the polarization strain field (6)–(7), with (8), for our three-dimensional composites to find

$$\begin{aligned}
K^{\text{eff}} &= \frac{\langle \sigma_{ii} \rangle}{3\langle \varepsilon_{ii} \rangle} = \frac{\sum_{\alpha=1}^{n} v_\alpha \langle \sigma_{ii} \rangle_\alpha}{3 \sum_{\alpha=1}^{n} v_\alpha \langle \varepsilon_{ii} \rangle_\alpha} = \frac{\sum_{\alpha=1}^{n} v_\alpha 3K_\alpha \langle \varepsilon_{ii} \rangle_\alpha}{3 \sum_{\alpha=1}^{n} v_\alpha \langle \varepsilon_{ii} \rangle_\alpha}\\
&= \frac{1}{\varepsilon^0_{ii}} \left(3 \sum_{\alpha=1}^{n} \frac{v_\alpha K_\alpha}{K_\alpha + K_*} \left(\sum_{\beta=1}^{n} \frac{v_\beta}{K_\beta + K_*} \right)^{-1} \varepsilon^0_{ii} \right) = \left(\sum_{\alpha=1}^{n} \frac{v_\alpha}{K_\alpha + K_*} \right)^{-1} - K_*.
\end{aligned} \tag{10}$$

Alternatively, instead of (6), one may use the polarization stress field (9) as the approximate field to find the approximation identical to (10). This is quite interesting, as the upper and lower bounds found in [Pham 1993] do not coincide. Indeed, the approximate fields (6) and (9) found from the upper- and lower-bound approaches without submitting to the minimum energy principles still cannot provide the precise information of whether they would help approximate the exact effective bulk modulus from above or below. They themselves only give some rough approximations involving some free parameters. Combining the two-dimensional case of [Tran and Pham 2015] and the three-dimensional case here, the estimation can be given in the general form (in d-dimensional space with $d = 2, 3$)

$$K^{\text{eff}} = P^{(n)}_K(K_*) = \left(\sum_{\alpha=1}^{n} \frac{v_\alpha}{K_\alpha + K_*} \right)^{-1} - K_*, \quad K_*(\mu_0) = \frac{2(d-1)}{d} \mu_0. \tag{11}$$

The estimation (11) has a feature that the property function $P^{(n)}_K(K_*)$ is a positive monotonously increasing function with respect to the positive parameter K_*, and it falls within HS bounds

$$\begin{aligned}
&P^{(n)}_K(K_{*\min}) \le K^{\text{eff}} \le P^{(n)}_K(K_{*\max}),\\
&K_{*\min} = K_*(\mu_{\min}), \quad \mu_{\min} = \min\{\mu_1, \ldots, \mu_n\},\\
&K_{*\max} = K_*(\mu_{\max}), \quad \mu_{\max} = \max\{\mu_1, \ldots, \mu_n\},
\end{aligned} \tag{12}$$

where $K_*(\mu_0)$ is defined in (11), when

$$K_{*\min} \le K_* \le K_{*\max}, \tag{13}$$

and vice versa.

The remaining free parameter K_* of the estimation (11) should be determined from a reference macroscopic bulk modulus of the composite at certain reference volume proportions v_α of the component materials. Should the reference macroscopic bulk modulus at some reference volume proportions of the components satisfy HS bounds, the respective reference parameter K_* would fall inside the interval bounded by $K_{*\min}$ and $K_{*\max}$. Then with that particular value K_* the estimation (11) shall obey HS bounds over all the volume proportions v_α of the component materials. Equation (11) shall be formally referred to as the polarization approximation (PA) for the effective elastic bulk modulus of the isotropic n-component material in the d-dimensional space.

Similarly, to find the approximation for the effective elastic shear modulus μ^{eff}, we again use the polarization strain field (6) to obtain

$$\begin{aligned}\mu^{\text{eff}} &= \frac{\langle\sigma_{12}\rangle}{2\langle\varepsilon_{12}\rangle} = \frac{\sum_{\alpha=1}^n v_\alpha 2\mu_\alpha\langle\varepsilon_{12}\rangle_\alpha}{2\sum_{\alpha=1}^n v_\alpha\langle\varepsilon_{12}\rangle_\alpha} \\ &= \frac{1}{\varepsilon_{12}^0}\left(\sum_{\alpha=1}^n \frac{2v_\alpha\mu_\alpha}{\mu_\alpha+\mu_*}\left(\sum_{\beta=1}^n \frac{v_\beta}{\mu_\beta+\mu_*}\right)^{-1}\varepsilon_{12}^0\right) = \left(\sum_{\alpha=1}^n \frac{v_\alpha}{\mu_\alpha+\mu_*}\right)^{-1} - \mu_*. \end{aligned} \tag{14}$$

Alternatively, the same estimation (14) can also be obtained starting from the polarization stress field (9).

Combining the two-dimensional case of [Tran and Pham 2015] and the three-dimensional case here, generally, in d-dimensional space ($d = 2, 3$), the estimation for μ^{eff} can be given in the form

$$\begin{aligned}\mu^{\text{eff}} = P_\mu^{(n)}(\mu_*) &= \left(\sum_{\alpha=1}^n \frac{v_\alpha}{\mu_\alpha+\mu_*}\right)^{-1} - \mu_*, \\ \mu_*(K_0,\mu_0) &= \mu_0\frac{d^2K_0 + 2(d+1)(d-2)\mu_0}{2dK_0 + 4d\mu_0},\end{aligned} \tag{15}$$

which falls inside HS bounds

$$\begin{aligned} P_\mu^{(n)}(\mu_{*\min}) \le \mu^{\text{eff}} \le P_\mu^{(n)}(\mu_{*\max}), \\ \mu_{*\min} = \mu_*(K_{\min},\mu_{\min}), \quad K_{\min} = \min\{K_1,\dots,K_n\}, \\ \mu_{*\max} = \mu_*(K_{\max},\mu_{\max}), \quad K_{\max} = \max\{K_1,\dots,K_n\}, \end{aligned} \tag{16}$$

where $\mu_*(K_0,\mu_0)$ is defined in (15) and $\mu_{\min}$ and $\mu_{\max}$ are defined in (12), when

$$\mu_{*\min} \le \mu_* \le \mu_{*\max}. \tag{17}$$

Similarly as in the case of the bulk modulus, the remaining free parameter μ_* of estimation (15) should be determined from a reference macroscopic shear modulus of the composite at certain reference volume proportions v_α of the component materials. Should the reference macroscopic shear modulus at some reference volume proportions of the components satisfy HS bounds, the respective reference parameter μ_* would fall inside the interval bounded by $\mu_{*\min}$ and $\mu_{*\max}$. Then with that particular

value μ_* the estimation (15) shall obey HS bounds over all the volume proportions v_α of the component materials. Equation (15) shall be referred to as the PA for the effective elastic shear modulus of the isotropic n-component material in d-dimensional space.

3. Reference at dilute suspension of the inclusions

Many EMAs are based on analytical Eshelby theoretical dilute solution results for an ellipsoidal inclusion suspended in an infinite matrix. So firstly, we construct a polarization approximation using the dilute solution reference. Let us consider the n-component matrix composite that is composed of the matrix component with $v_1 = v_M$, $K_1 = K_M$, and $\mu_1 = \mu_M$ and the inclusion components with v_α, K_α, and μ_α ($\alpha = 2, \ldots, n$). We may take the reference model for the composite as that at dilute suspensions of the same-geometry inclusions with the moduli K_α and μ_α and volume fractions tv_α ($\alpha = 2, \ldots, n$ and $t \ll 1$) in the matrix of moduli K_M and μ_M. Let the respective dilute solution results have the forms

$$K^{\text{eff}} = K_M + \sum_{\alpha=2}^{n} t v_\alpha (K_\alpha - K_M) D_{K\alpha}(K_\alpha, \mu_\alpha, K_M, \mu_M), \quad t \ll 1, \tag{18}$$

$$\mu^{\text{eff}} = \mu_M + \sum_{\alpha=2}^{n} t v_\alpha (\mu_\alpha - \mu_M) D_{\mu\alpha}(K_\alpha, \mu_\alpha, K_M, \mu_M), \quad t \ll 1, \tag{19}$$

where $D_{K\alpha}$ and $D_{\mu\alpha}$ are inclusion functions depending on the α-inclusion component's geometry; their values can be found analytically, numerically, or even experimentally. At that dilute limit, our polarization approximations (11) and (15) have the respective asymptotic expressions

$$K^{\text{eff}} = K_M + \sum_{\alpha=2}^{n} t v_\alpha (K_\alpha - K_M) \frac{K_M + K_*}{K_\alpha + K_*}, \quad t \ll 1, \tag{20}$$

$$\mu^{\text{eff}} = \mu_M + \sum_{\alpha=2}^{n} t v_\alpha (\mu_\alpha - \mu_M) \frac{\mu_M + \mu_*}{\mu_\alpha + \mu_*}, \quad t \ll 1. \tag{21}$$

Equalizing (18) with (20) and (19) with (21), respectively, one obtains the equations determining the reference parameters K_* and μ_* separately:

$$\sum_{\alpha=2}^{n} v_\alpha (K_\alpha - K_M) \left[\frac{K_M + K_*}{K_\alpha + K_*} - D_{K\alpha}(K_\alpha, \mu_\alpha, K_M, \mu_M) \right] = 0, \tag{22}$$

$$\sum_{\alpha=2}^{n} v_\alpha (\mu_\alpha - \mu_M) \left[\frac{\mu_M + \mu_*}{\mu_\alpha + \mu_*} - D_{\mu\alpha}(K_\alpha, \mu_\alpha, K_M, \mu_M) \right] = 0. \tag{23}$$

Equation (11), with K_* determined from (22), and (15), with μ_* determined from (23), are our polarization approximations for the effective moduli of the matrix composite, using the dilute solution result reference (denoted further as PA0).

In the two-component case, with inclusion functions $D_K = D_K(K_I, \mu_I, K_M, \mu_M)$ and $D_\mu = D_\mu(K_I, \mu_I, K_M, \mu_M)$, (22) and (23) are solved explicitly:

$$K_* = \frac{D_K(K_I, \mu_I, K_M, \mu_M)K_I - K_M}{1 - D_K(K_I, \mu_I, K_M, \mu_M)}, \tag{24}$$

$$\mu_* = \frac{D_\mu(K_I, \mu_I, K_M, \mu_M)\mu_I - \mu_M}{1 - D_\mu(K_I, \mu_I, K_M, \mu_M)}. \tag{25}$$

Analytical expressions of the inclusion-associated functions $D_K(K_I, \mu_I, K_M, \mu_M)$ and $D_\mu(K_I, \mu_I, K_M, \mu_M)$ for 3D ellipsoidal and 2D elliptic inclusions have been constructed by Eshelby. They can be given in the form [Mura 1987; Torquato 2002]

$$D_K = \frac{1}{d} D^0_{iijj}, \qquad D_\mu = \frac{d}{d^2 + d - 2}\left(D^0_{ijij} - \frac{1}{d} D^0_{iijj}\right), \tag{26}$$

where

$$\boldsymbol{D}^0 = [\boldsymbol{I} + \boldsymbol{P} : \boldsymbol{C}_M^{-1} : (\boldsymbol{C}_I - \boldsymbol{C}_M)]^{-1}, \quad \boldsymbol{C}_I = \boldsymbol{T}(K_I, \mu_I),\ \boldsymbol{C}_M = \boldsymbol{T}(K_M, \mu_M) \tag{27}$$

and $\boldsymbol{P}$ is the fourth-rank Eshelby tensor. Particular expressions of the components of the tensors in two- and three-dimensional spaces are given in [Mura 1987].

The expressions of the inclusion-associated functions $D_K(K_I, \mu_I, K_M, \mu_M)$ and $D_\mu = D_\mu(K_I, \mu_I, K_M, \mu_M)$ for spherical (or circular) inclusions in general d-dimensional space are simply

$$D_K = \frac{K_M + K_{*M}}{K_I + K_{*M}}, \quad K_{*M} = K_*(\mu_M), \tag{28}$$

$$D_\mu = \frac{\mu_M + \mu_{*M}}{\mu_I + \mu_{*M}}, \quad \mu_{*M} = \mu_*(K_M, \mu_M), \tag{29}$$

where $K_*(\mu_0)$ and $\mu_*(K_0, \mu_0)$ are defined in (11) and (15), respectively. Then the solution of (20) with (28) and that of (21) with (29) should be $K_* = K_{*M}$ and $\mu_* = \mu_{*M}$, respectively (correspondingly, $K_0 = K_M$ and $\mu_0 = \mu_M$). Thus, we obtain the polarization approximation using the dilute solution result reference (PA0) for the n-component matrix composites with spherical inclusions in general d-dimensional space:

$$K^{\text{eff}} = P_K^{(n)}(K_{*M}), \qquad \mu^{\text{eff}} = P_\mu^{(n)}(\mu_{*M}), \tag{30}$$

which coincide with the Maxwell and Mori–Tanaka approximations [Torquato 2002] in that specific case.

Later we shall apply, among others, PA0 from (20)–(27) to matrix composites with noncircular inclusions. It appears that the results of PA0 for the two-component matrix composites with elliptic inclusions also coincide with those of the Mori–Tanaka approximation (as in the case of Figure 3). However, they generally differ for n-component matrix composites if $n \geq 3$ (as in the three-component case of Figure 4), except for the specific pure spherical-circular inclusion composites (30). That is expected, since the Mori–Tanaka approximation for three-component composites may violate Hashin–Shtrikman bounds [Norris 1989], while our polarization approximations, including PA0, by their construction, always obey the bounds.

4. Reference at finite volume proportions of the component materials

The reference parameters K_* and μ_* can be found from the dilute suspension results for the inclusions as was done in the previous section. Otherwise, the reference parameters can be determined, once the respective reference macroscopic moduli of a composite are available numerically or experimentally at any finite volume proportions of the component materials, for the approximations (11) and (15) to fit those reference macroscopic moduli. The resulting polarization approximations are called PA1.

For numerical illustrations, we consider some simple two-dimensional hexagonal-symmetry periodic microstructures, which have macroscopically isotropic elastic moduli, in Figures 1–4. Highly accurate numerical boundary element results used in Figure 1 have been taken from [Eischen and Torquato 1993], where $K_1 = K_M = 1$, $\mu_1 = \mu_M = 0.3$, $K_2 = K_I = 67.5$, and $\mu_2 = \mu_I = 40.5$. Standard periodic boundary conditions with finite element realizations have been used in Figures 2–4. Three periodic cells are indicated at the top of Figures 1–4.

For two-component composites of Figures 2–3, we take $K_1 = K_M = 1$, $\mu_1 = \mu_M = 0.4$, $K_2 = K_I = 20$, and $\mu_2 = \mu_I = 12$ (K_M is normalized to be unity). Figures 1 and 2 involve circular-inclusion composites, while the elliptic inclusions of Figures 3 and 4 have the aspect ratio $a_1 : a_2 = 2$.

In Figures 1–3 we compare graphics of effective elastic moduli of the respective two-component

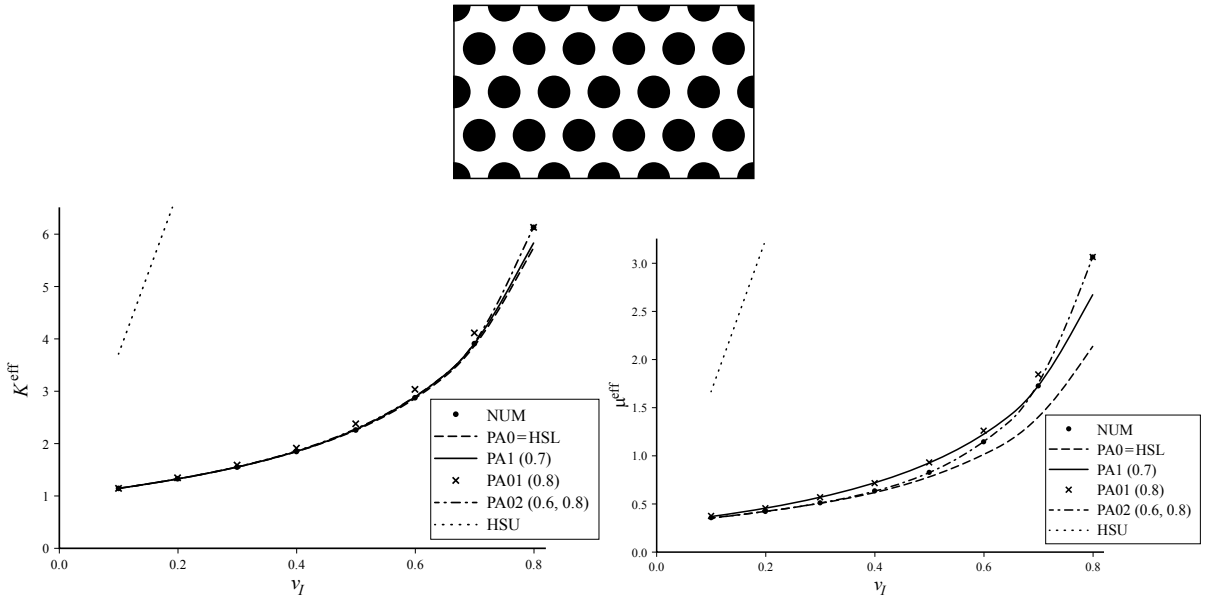

Figure 1. Effective elastic moduli of a 2D periodic circular-inclusion composite at a range of inclusion volumes v_I, with $K_M = 1$, $\mu_M = 0.3$, $K_I = 135$, and $\mu_I = 81$: numerical results (NUM) are compared with HS upper (HSU) and lower (HSL) bounds and polarization approximations PA0 using dilute solution reference, PA1(0.7) using the reference at $v_I = 0.7$, PA02(0.6, 0.8) using dilute solution reference and two references at $v_{I1} = 0.6$ and $v_{I2} = 0.8$, and PA01(0.8) using dilute solution reference and the reference at $v_I = 0.8$. Top: microstructure. Left: bulk modulus. Right: shear modulus.

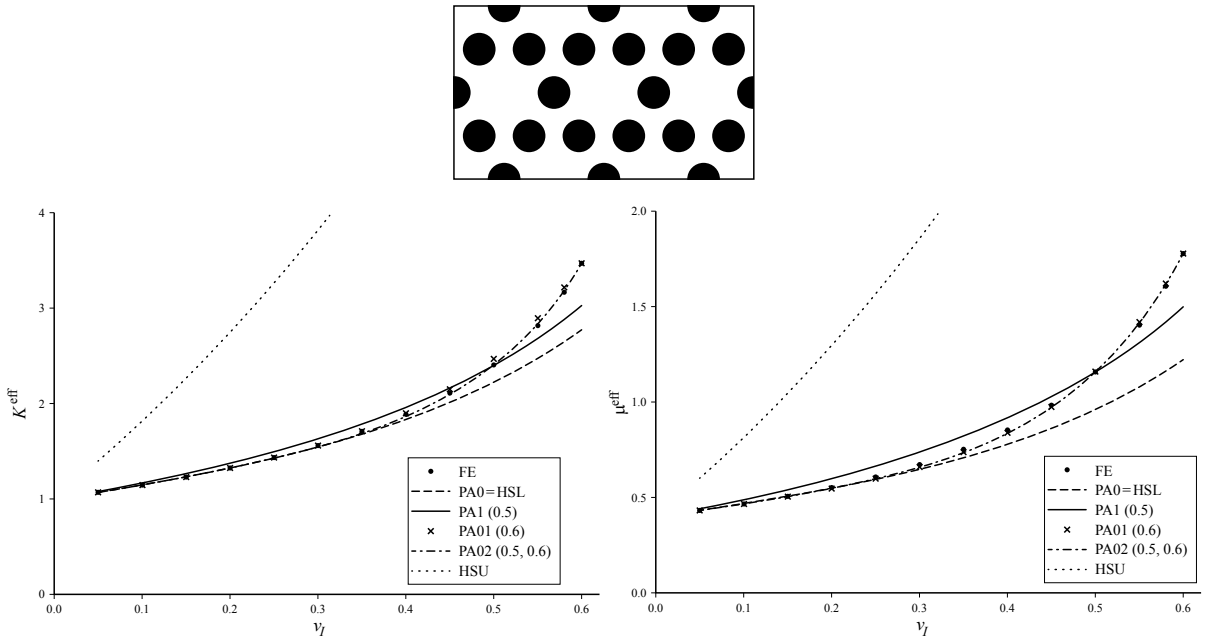

Figure 2. The moduli of another 2D periodic circular-inclusion composite (the data and notation as in Figure 1): FE are compared with HSU and HSL, PA0, PA1(0.5), PA02(0.5, 0.6), and PA01(0.6). Top: microstructure. Left: bulk modulus. Right: shear modulus.

composites calculated numerically (NUM or FE) with the Hashin–Shtrikman upper (HSU) and lower (HSL) bounds and our polarization approximations PA0, using the dilute suspension reference results, and PA1, using the reference at some finite volume proportions of the inclusion component, over large ranges of the inclusion phase $v_1 = v_I$. PA1(0.7), for example, indicates PA1 using the reference at $v_I = v_I^{\text{ref}} = 0.7$.

In Figures 1 and 2 with circular inclusions, PA0 coincides with HSL, Maxwell, and Mori–Tanaka approximations, as noted in the previous section. However, PA0 using the dilute elliptic-inclusion reference results from (22)–(23) and (26)–(27) in Figure 3 (as well as PA0 of Figure 4) differs from HS bounds.

One may observe that all PA0 and PA1 fall within HS bounds as expected. PA1, using the reference at finite volume proportion of the included phases, approximates the numerical results better than PA0, using the dilute suspension reference results, over certain finite volume ranges of the included phases (especially near the reference points). The results also reveal that, for the two-component matrix composites, PA0 seems to give lower estimates of the effective moduli, while PA1 provides lower estimates at $v_I > v_I^{\text{ref}}$ and upper estimates at $v_I < v_I^{\text{ref}}$ if the inclusion phase is stiffer than the matrix phase and vice versa if the matrix phase is stiffer (we do not show the respective graphs in the case that the matrix phase is stiffer, because the differences between the curves NUM, FE, HSU, PA0, and PA1 are much less significant there, and we do not want to overload the paper with additional figures).

Our approximations apply to general multicomponent materials. In Figure 4 a three-component composite is considered. Again $K_1 = K_M = 1$ and $\mu_1 = \mu_M = 0.4$, and we take $K_2 = 10$ and $\mu_2 = 6$

(dark elliptic inclusions) and $K_3 = 0.2$ and $\mu_3 = 0.1$ (gray circular inclusions). FE, HSU, HSL, PA0, and PA1 results are compared in Figure 4 over a range of volume proportions of the included phases $v_I = v_2 + v_3$ (presume $v_2 = v_3$).

Experimentally measured values of the macroscopic elastic moduli of a composite at certain volume fractions of the component materials can also serve as the reference moduli for our polarization approximation for the composite over all the ranges of volume fractions of the component materials. Experimental data on the compressibility (elastic bulk modulus) of the porous glass over a range of porosity v_I reported in [Walsh et al. 1965] is displayed in Figure 5. The elastic moduli of the glass are $K_M = 46.3\,\text{GPa}$ and $\mu_M = 30.5\,\text{GPa}$. PA1 for the macroscopic bulk modulus corresponding to an experimental reference point and the HS upper bound are given in the figure for comparisons (HS lower bound is identically zero in this case). The notation PA1(6) denotes PA1 corresponding to the experimental reference point 6 in the graph.

Experimental data on the macroscopic elastic Young's modulus E^{eff} and Poisson's ratio ν^{eff} of a particulate-filled glassy polymer [Smith 1976] is displayed in Figure 6, top row. The elastic constants of the polymer matrix are $E_M = 3.01\,\text{GPa}$ and $\nu_M = 0.394$, while those for the glass are $E_I = 76\,\text{GPa}$ and $\nu_I = 0.23$. The relations between the 3D elastic constants E, ν, K, and μ are

$$K = \frac{E}{3(1-2\nu)}, \quad \mu = \frac{E}{2(1+\nu)}, \quad E = \frac{9K\mu}{3K+\mu}, \quad \nu = \frac{3K-2\mu}{6K+2\mu}. \tag{31}$$

Figure 6 shows PAs for the macroscopic elastic constants corresponding to various experimental reference points and HS bounds.

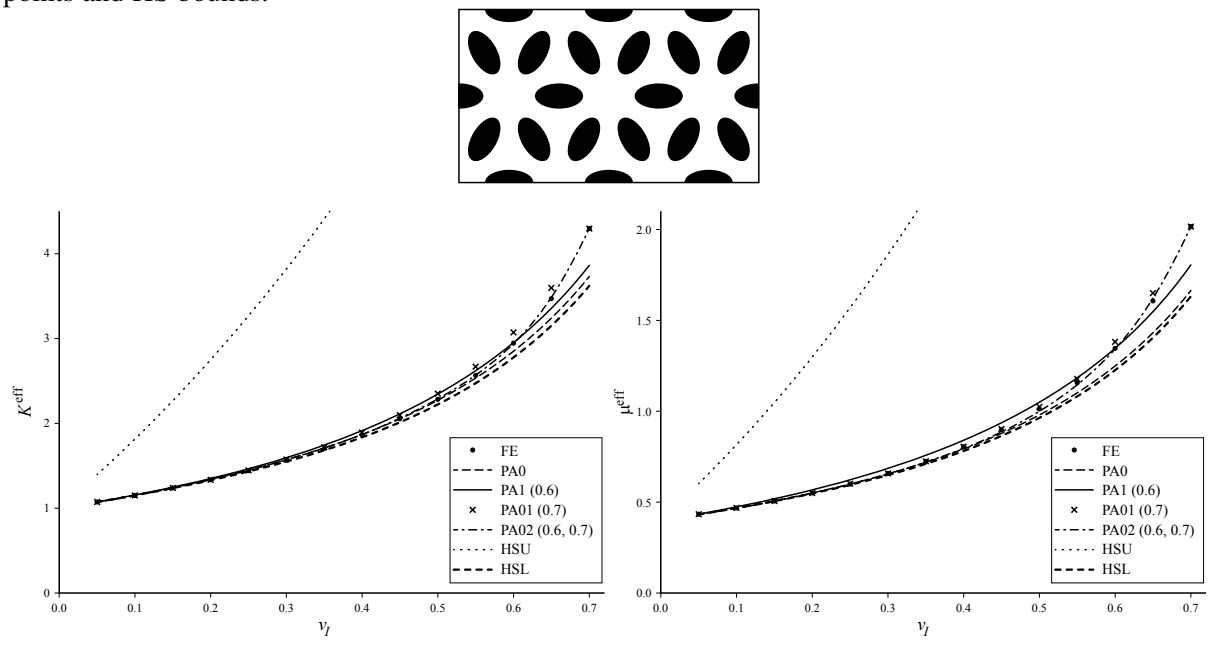

Figure 3. The moduli of a 2D periodic elliptic-inclusion composite (the data and notation as in Figure 1), and the aspect ratio of the ellipses is 2: FE are compared with HS bounds, PA0, PA1(0.6), PA02(0.6, 0.7), and PA01(0.7). Top: microstructure. Left: bulk modulus. Right: shear modulus.

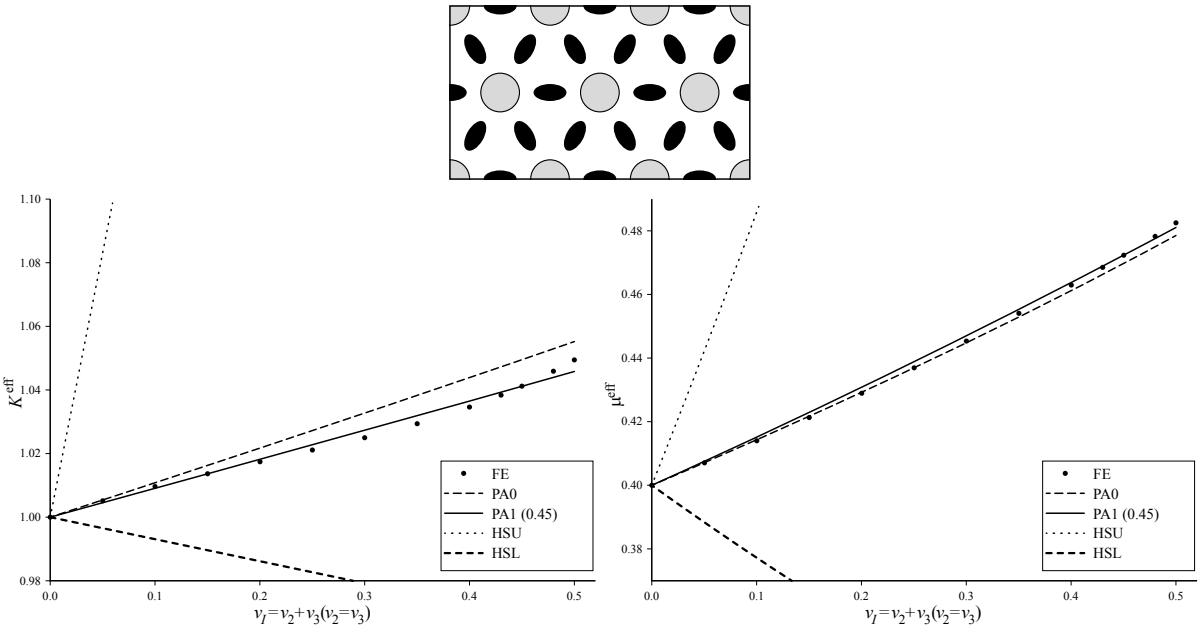

Figure 4. The moduli of a 2D three-component periodic elliptic-circular-inclusion composite at a range of inclusion volumes $v_I = v_2 + v_3$, $v_2 = v_3$, with $K_1 = K_M = 1$ and $\mu_1 = \mu_M = 0.4$ and $K_2 = 10$ and $\mu_2 = 6$ (dark elliptic inclusions) or $K_3 = 0.2$ and $\mu_3 = 0.1$ (gray circular inclusions), and the aspect ratio of the ellipses is 2: FE are compared with HS bounds, PA0, and PA1(0.45). Top: microstructure. Left: bulk modulus. Right: shear modulus.

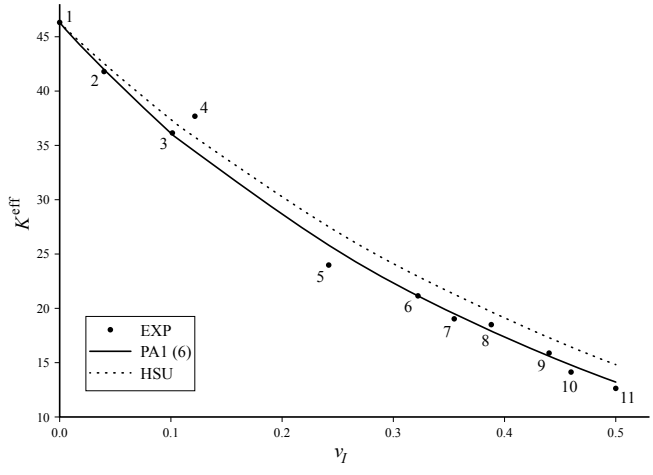

Figure 5. Macroscopic elastic bulk modulus of a porous glass over a range of porosity v_I; the elastic moduli of the glass are $K_M = 46.3\,\text{GPa}$ and $\mu_M = 30.5\,\text{GPa}$. Experimental data (EXP) are compared with HSU (HSL is identically zero) and PA1(6) using the reference at the reference experimental point 6.

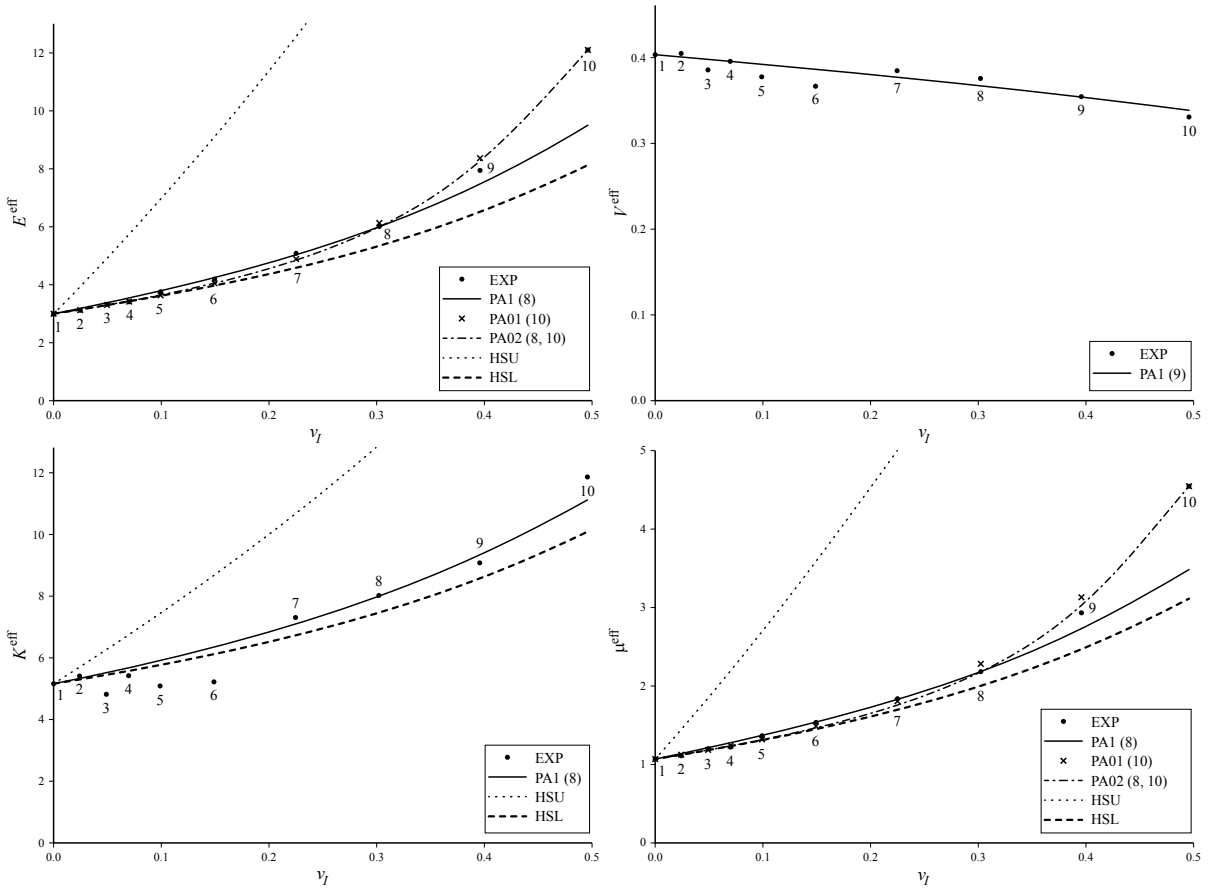

Figure 6. Macroscopic elastic constants of a particulate-filled glassy polymer over a range of inclusion volumes v_I; the elastic constants of the polymer matrix are $E_M = 3.01\,\text{GPa}$ and $\nu_M = 0.394$, while those for the glass are $E_I = 76\,\text{GPa}$ and $\nu_I = 0.23$. Experimental data (EXP) are compared with HS bounds, PA1, PA02, and PA01 using the references at the indicated reference experimental points. Top left: Young's modulus. Top right: Poisson's ratio. Bottom left: bulk modulus. Bottom right: shear modulus.

With a one-point reference parameter reflecting the feature of the microgeometry of a particular composite, as with many other EMAs, the polarization approximations PA0 and PA1 have inevitable limitations. For high-contrast-component-property composites, at finite volume proportions of the inclusions, the approximations yield good results only near the reference point and the results become poorer with increasing distance from the reference point. Even so, they should obey HS bounds over all the ranges of component proportions, once the reference model satisfies HS bounds at the reference point.

5. Multipoint polarization approximations

By assuming K_* and μ_* are functions of volume proportions of the component materials, we are able to use more reference points to obtain better approximations of the effective moduli. The variable reference

parameters K_* and μ_* should lie within the intervals (13) and (17), respectively, for the approximations to obey HS bounds.

Further, in the remaining part of this paper, we shall restrict ourselves to two-component materials and assume the variable reference parameters K_* and μ_* of the polarization approximations (11) and (15), respectively, to be of the form

$$K_* = \bar{K}_*(c + a v_2^b), \qquad b > 0, \tag{32}$$

$$\mu_* = \bar{\mu}_*(c' + a' v_2^{b'}), \quad b' > 0, \tag{33}$$

where $\bar{K}_*$ and $\bar{\mu}_*$ are some fixed values of elastic moduli dimension; three dimensionless parameters a, b, c or a', b', c' should be found from appropriate available references. Presume we have three numerical or experimental reference values of the effective elasticity $K^{\text{eff}} = K^{\text{eff}}_{\text{ref}\,1}, K^{\text{eff}}_{\text{ref}\,2}, K^{\text{eff}}_{\text{ref}\,3}$ and $\mu^{\text{eff}} = \mu^{\text{eff}}_{\text{ref}\,1}, \mu^{\text{eff}}_{\text{ref}\,2}, \mu^{\text{eff}}_{\text{ref}\,3}$ at the volume proportions $v_2 = v_{21}, v_{22}, v_{23}$, respectively. Solving (11) in the two-component case, one finds

$$K_*^{\text{ref}} = \frac{K^{\text{eff}}_{\text{ref}}(v_1 K_2 + v_2 K_1) - K_1 K_2}{v_1 K_1 + v_2 K_2 - K^{\text{eff}}_{\text{ref}}} \tag{34}$$

and the respective values of the reference parameter $K^{\text{ref}}_{*1}, K^{\text{ref}}_{*2}, K^{\text{ref}}_{*3}$ corresponding to $K^{\text{eff}}_{\text{ref}\,1}, K^{\text{eff}}_{\text{ref}\,2}, K^{\text{eff}}_{\text{ref}\,3}$. Now with (32) one derives three dimensionless equations for three dimensionless parameters a, b, c:

$$(c + a v_{21}^b) = k_1, \qquad (c + a v_{22}^b) = k_2, \qquad (c + a v_{23}^b) = k_3, \tag{35}$$

where

$$k_1 = K^{\text{ref}}_{*1}/\bar{K}_*, \qquad k_2 = K^{\text{ref}}_{*2}/\bar{K}_*, \qquad k_3 = K^{\text{ref}}_{*3}/\bar{K}_*. \tag{36}$$

Equation (35) leads to the unique equation determining b

$$\frac{v_{21}^b - v_{22}^b}{v_{21}^b - v_{23}^b} = \frac{k_1 - k_2}{k_1 - k_3}, \tag{37}$$

and explicit expressions for a and c

$$a = \frac{k_1 - k_2}{v_{21}^b - v_{22}^b}, \qquad c = k_1 - a v_{21}^b. \tag{38}$$

The polarization approximations (11) and (32) for K^{eff} with the parameters a, b, c determined from (37)–(38) shall be referred to as three-point polarization approximation PA3. Since K_* in (32) is a monotonous function of v_2, if the reference macroscopic moduli $K^{\text{eff}}_{\text{ref}\,1}, K^{\text{eff}}_{\text{ref}\,2}, K^{\text{eff}}_{\text{ref}\,3}$ satisfy HS bounds, the approximations (11) and (38) also obey HS bounds, at least, over the range $\min\{v_{21}, v_{22}, v_{23}\} \le v_2 \le \max\{v_{21}, v_{22}, v_{23}\}$. Independently, a similar three-point polarization approximation for μ^{eff} from (15) and (33) is obtained. The respective equations (34)–(38) keep the same forms, except that one has to substitute notations μ, a', b', c' for K, a, b, c.

In the case of two-component matrix composites, with the notation $v_1 = v_M$, $K_1 = K_M$, $\mu_1 = \mu_M$, and $v_2 = v_I$, $K_2 = K_I$, $\mu_2 = \mu_I$, if dilute solution results (18)–(19) are available, one can use them to find c and c' independently as was done in Section 3 and suggest simpler two-point polarization approximations

(11) for K^{eff} and (15) for μ^{eff} with variable reference parameters involving just two free parameters a and b (and a' and b'):

$$K_* = \overline{K}_*(1 + a v_2^b), \quad \overline{K}_* = \frac{D_K K_I - K_M}{1 - D_K}, \tag{39}$$

$$\mu_* = \bar{\mu}_*(1 + a' v_2^{b'}), \quad \bar{\mu}_* = \frac{D_\mu \mu_I - \mu_M}{1 - D_\mu}, \tag{40}$$

where D_K and D_μ are the functions from the dilute solution results (27)–(28) which have the expressions (26)–(27) for ellipsoidal (elliptic) inclusion cases. Now one needs just two reference equations determining a and b:

$$1 + a v_{21}^b = k_1, \qquad 1 + a v_{22}^b = k_2. \tag{41}$$

Equation (41) can be solved explicitly to give

$$b = \log_{v_{21}/v_{22}} \frac{k_1 - 1}{k_2 - 1} = \ln \frac{k_1 - 1}{k_2 - 1} \Big/ \ln \frac{v_{21}}{v_{22}}, \quad a = \frac{k_1 - 1}{v_{21}^b}. \tag{42}$$

Polarization approximations (11), (39), (41), and (42) using the dilute solution reference and two references at $v_2 = v_{21}, v_{22}$ is referred to as PA02. Independently, a similar polarization approximation PA02 for μ^{eff} from (15) and (40) is obtained. The respective equations (41)–(42) keep the same forms, with the only change being the substitution of the notations μ, a', b', c' for K, a, b, c. One observes that the approximations obey HS bounds, at least, over the range $0 \le v_2 \le \max\{v_{21}, v_{22}\}$.

Graphs of PA02 from (11), (15), (39)–(42), and (26) for the suspension of elliptic inclusions of the configuration of Figure 3, top, using the dilute solution result and two numerical references at $v_{I1} = 0.6$ and $v_{I2} = 0.7$, are presented with $a = 27.6$ and $b = 9.75$ (Figure 3, left) and $a' = 8.17$ and $b' = 6.11$ (Figure 3, right). One can observe that PA02 fits well with the numerical data.

In the case of composites with sphere-like (circular-like) inclusions, D_K and D_μ have simple expressions (28)–(29), and $\overline{K}_* = K_*(\mu_M)$ and $\bar{\mu}_* = \mu_*(K_M, \mu_M)$ in (39) and (40). Applications of PA02 are presented with numerical references at $v_{I1} = 0.6$ and $v_{I2} = 0.8$ and $a = 3.17$ and $b = 9.43$ (Figure 1, left) and $a' = 3.18$ and $b' = 3.60$ (Figure 1, right). Similarly PA02 is given with numerical references at $v_{I1} = 0.5$ and $v_{I2} = 0.6$ and $a = 32.5$ and $b = 5.72$ (Figure 2, left) and $a' = 19$ and $b' = 4.08$ (Figure 2, right). PA02 with experimental references at the experimental points 8 and 10 are shown with $a = 10.5$ and $b = 2.34$ (Figure 6, top left) and $a' = 12.5$ and $b' = 2.9$ (Figure 6, bottom right). In all the cases, PA02 fits the numerical or experimental data much better than PA0 or PA1, as expected.

If only one numerical or experimental value of the effective moduli of the matrix composite at a finite volume proportion point $v_2 = v_I = v_{I1}$ is available for reference (in addition to the dilute solution one), one has to fix an additional parameter, for instance b or b', and obtains just one equation (the first one of (41)) which determines the remaining parameter a or a', according to the second equation of (42). The resulted approximation is called PA01. It should obey HS bounds, at least, over the range $0 \le v_I \le v_{I1}$.

PA01 with $b = b' = 4$ is projected using numerical reference at $v_{I1} = 0.6$ and $a = 13.5$ (Figure 2, left) or $a' = 18.2$ (Figure 2, right) and at $v_{I1} = 0.7$ and $a = 3.55$ (Figure 3, left) or $a' = 3.85$ (Figure 3, right). PA01 with $b = b' = 2$ is applied using numerical reference at $v_{I1} = 0.8$ and $a = 0.606$ (Figure 1, left) and $a' = 0.227$ (Figure 1, right) and with experimental reference at the experimental point 10 and $a = 8.31$ (Figure 6, top left) or $a' = 6.68$ (Figure 6, bottom right). Though b and b' for PA01 in those

figures are chosen to be not quite close to the respective b and b' for PA02, the approximations appear relatively good.

6. Conclusion

Unlike other EMAs (such as the self-consistent, differential, Maxwell, and Mori–Tanaka ones), which are constructed from the field equations, our PAs are based on the approximate field solutions which come from minimum energy principles. The "optimal" polarization trial fields constructed earlier to bound the effective elastic moduli of isotropic multicomponent materials have been implemented to derive the PAs for the moduli in three and generally d dimensions. The approximations are separate functions for the effective bulk and shear moduli and contain, in addition to the moduli and volume proportions of the components, certain free parameters, which should be determined from some reference effective moduli at certain volume proportions of the component materials analytically, numerically, or experimentally. Specifically, PA0 using the dilute solution reference (similar to other EMAs) as well as PA1 using the reference at a component's finite volume proportion point should obey HS bounds over all the ranges of volume proportions of the component materials. Refined approximations with variable reference parameters incorporating more available information about a particular composite should improve the accuracy of the estimations. Specifically, PA02 using dilute solution reference and two references at components' finite volume proportion points and PA01 using dilute solution reference and one reference at a component's finite volume proportion point can yield good approximations. The approximations satisfy HS bounds, at least, over the volume proportion range between the extreme reference points.

Acknowledgment

This study is supported by Vietnam's National Foundation for Science and Technology Development, project 107.02-2014.08.

References

[Christensen 1979] R. M. Christensen, *Mechanics of composite materials*, Wiley, New York, 1979.

[Eischen and Torquato 1993] J. W. Eischen and S. Torquato, "Determining elastic behavior of composites by the boundary element method", *J. Appl. Phys.* **74**:1 (1993), 159–170.

[Eshelby 1957] J. D. Eshelby, "The determination of the elastic field of an ellipsoidal inclusion, and related problems", *Proc. Roy. Soc. London. A* **241** (1957), 376–396.

[Franciosi et al. 2011] P. Franciosi, R. Brenner, and A. El Omri, "Effective property estimates for heterogeneous materials with cocontinuous phases", *J. Mech. Mater. Struct.* **6**:5 (2011), 729–763.

[Hashin and Shtrikman 1963] Z. Hashin and S. Shtrikman, "A variational approach to the theory of the elastic behaviour of multiphase materials", *J. Mech. Phys. Solids* **11**:2 (1963), 127–140.

[Klusemann et al. 2012] B. Klusemann, H. J. Böhm, and B. Svendsen, "Homogenization methods for multi-phase elastic composites with non-elliptical reinforcements: comparisons and benchmarks", *Eur. J. Mech. A* **34** (2012), 21–37.

[Kushch et al. 2013] V. I. Kushch, S. G. Mogilevskaya, H. K. Stolarski, and S. L. Crouch, "Evaluation of the effective elastic moduli of particulate composites based on Maxwell's concept of equivalent inhomogeneity: microstructure-induced anisotropy", *J. Mech. Mater. Struct.* **8**:5–7 (2013), 283–303.

[Milton 2002] G. W. Milton, *The theory of composites*, Cambridge Monographs on Applied and Computational Mathematics **6**, Cambridge University, 2002.

[Mogilevskaya et al. 2012] S. G. Mogilevskaya, H. K. Stolarski, and S. L. Crouch, "On Maxwell's concept of equivalent inhomogeneity: when do the interactions matter?", *J. Mech. Phys. Solids* **60**:3 (2012), 391–417.

[Mori and Tanaka 1973] T. Mori and K. Tanaka, "Average stress in matrix and average elastic energy of materials with misfitting inclusions", *Acta Metall.* **21**:5 (1973), 571–574.

[Mura 1987] T. Mura, *Micromechanics of defects in solids*, 2nd ed., Mechanics of Elastic and Inelastic Solids **3**, Kluwer, Dordrecht, 1987.

[Nogales and Böhm 2008] S. Nogales and H. J. Böhm, "Modeling of the thermal conductivity and thermomechanical behavior of diamond reinforced composites", *Int. J. Eng. Sci.* **46**:6 (2008), 606–619.

[Norris 1989] A. N. Norris, "An examination of the Mori–Tanaka effective medium approximation for multiphase composites", *ASME J. Appl. Mech.* **56**:1 (1989), 83–88.

[Pham 1993] D. C. Pham, "Bounds on the effective shear modulus of multiphase materials", *Int. J. Eng. Sci.* **31**:1 (1993), 11–17.

[Pham 2012] D. C. Pham, "Bounds on the elastic moduli of statistically isotropic multicomponent materials and random cell polycrystals", *Int. J. Solids Struct.* **49**:18 (2012), 2646–2659.

[Pham 2014] D. C. Pham, "Improved three-point correlation estimates for the effective elastic moduli of random orthorhombic crystals and multicomponent materials", *Philos. Mag. A* **94**:10 (2014), 1112–1131.

[Phan-Thien and Pham 2000] N. Phan-Thien and D. C. Pham, "Differential multiphase models for polydispersed spheroidal inclusions: thermal conductivity and effective viscosity", *Int. J. Eng. Sci.* **38**:1 (2000), 73–88.

[Sevostianov and Kachanov 2014] I. Sevostianov and M. Kachanov, "On some controversial issues in effective field approaches to the problem of the overall elastic properties", *Mech. Mater.* **69**:1 (2014), 93–105.

[Smith 1976] J. C. Smith, "Experimental values for the elastic constants of a particulate-filled glassy polymer", *J. Res. NBS A* **80A**:1 (1976), 45–49.

[Torquato 2002] S. Torquato, *Random heterogeneous materials: microstructure and macroscopic properties*, Interdisciplinary Applied Mathematics **16**, Springer, 2002.

[Tran and Pham 2015] A. B. Tran and D. C. Pham, "Polarization approximations for the macroscopic elastic constants of transversely isotropic multicomponent unidirectional fiber composites", *J. Compos. Mater.* **49**:30 (2015), 3765–3780.

[Walpole 1966] L. J. Walpole, "On bounds for the overall elastic moduli of inhomogeneous systems, I", *J. Mech. Phys. Solids* **14**:3 (1966), 151–162.

[Walsh et al. 1965] J. B. Walsh, W. F. Brace, and A. W. England, "Effect of porosity on compressibility of glass", *J. Am. Ceram. Soc.* **48**:12 (1965), 605–608.

[Willis 1977] J. R. Willis, "Bounds and self-consistent estimates for the overall properties of anisotropic composites", *J. Mech. Phys. Solids* **25**:3 (1977), 185–202.

Received 4 Jul 2016. Revised 5 Mar 2017. Accepted 27 Mar 2017.

DUC CHINH PHAM: pdchinh@imech.vast.vn
Institute of Mechanics, Vietnam Academy of Science and Technology, 264 Doi Can, Ba dinh, Hanoi, Vietnam

and

Graduate University of Science and Technology – VAST, 18 Hoang Quoc Viet, Hanoi, Vietnam

NGUYEN QUYET TRAN: tranquyetth@gmail.com
Department of Applied Mechanics, Hanoi University of Industry, 298 Cau Dien, Hanoi, Vietnam

and

Graduate University of Science and Technology – VAST, 18 Hoang Quoc Viet, Hanoi, Vietnam

ANH BINH TRAN: anh-binh.tran@nuce.edu.vn
Department of Applied Informatics in Construction, National University of Civil Engineering, 55 Giai phong, Hanoi, Vietnam

and

Graduate University of Science and Technology – VAST, 18 Hoang Quoc Viet, Hanoi, Vietnam

JOURNAL OF MECHANICS OF MATERIALS AND STRUCTURES

msp.org/jomms

Founded by Charles R. Steele and Marie-Louise Steele

See msp.org/jomms for submission guidelines.

JoMMS (ISSN 1559-3959) at Mathematical Sciences Publishers, 798 Evans Hall #6840, c/o University of California, Berkeley, CA 94720-3840, is published in 10 issues a year. The subscription price for 2017 is US $615/year for the electronic version, and $775/year (+$60, if shipping outside the US) for print and electronic. Subscriptions, requests for back issues, and changes of address should be sent to MSP.

JoMMS peer-review and production is managed by EditFLOW® from Mathematical Sciences Publishers.

PUBLISHED BY

mathematical sciences publishers

nonprofit scientific publishing

http://msp.org/

Journal of Mechanics of Materials and Structures

Volume 12, No. 4 July 2017

1559-3959(2017)12:4;1-1